An improved head form for use in helmet certification drop tests
a combined experimental and numerical approach

Plasmans, C.J.P.

Award date:
2000

Technische Universiteit Eindhoven
Department of Mechanical Engineering
Section of Engineering Dynamics and Biomechanics

An improved head form for use in helmet certification drop tests

-a combined experimental and numerical approach-

C.J.P. Plasmans

WFW-report 2000.08

Under supervision of:
Prof.dr.ir. D.H. van Campen
Dr.ir. A.A.H.J. Sauren
Ir. H.L.A. van den Bosch

"As far as the laws of mathematics refer to reality, they are not certain, as far as they are certain, they do not refer to reality." - *Albert Einstein*

∞

"Be happy. It's one way of being wise." - *Colette (French writer)*

Contents

Chapter 1

Scope of the project

1.1 General Introduction

The number of people who die as a result of traffic accidents is decreasing [1]. Passive safety measures such as passenger restraint systems, helmets, airbags and vehicle crush zones, as well as active safety measures such as anti-lock braking and improved visibility seem to be effective. However, injuries due to motor vehicle crashes remain one of the leading causes of death and disability [2]. In 1998 in The Netherlands 1066 people died as a result of traffic accidents, 76 of which were motor cyclists. Another 20,000 people required medical treatment [1]. Worldwide motor vehicle crashes cause about 500,000 road deaths annually.

Head injuries still remain critical in the automotive environment. Due to its anatomical structure the head is very susceptible to injuries and makes it the most frequently injured body part [3]: approximately 30% of the traffic accidents result in head injuries [4]. In order to reduce the amount of head injuries, particularly those of motor cyclists, in most countries the use of crash helmets is obligatory.

In practice, crash helmets have proven their effectiveness. Accident studies have shown that in a direct impact a head injury risk reduction of approximately 35% up to over 90% can be achieved [5]. This effectiveness is primarily due to a reduction of the head injury risk through their shock absorption capacity, however the exact manner in which they protect the head is unknown.
A powerful modelling tool in head injury reserach is the Finite Element Method (FEM). FEM models give access to field parameters possibly cor-

related to injuries, such as stress, strain and pressure, that often are experimentally difficult to measure. One shoul bear in mind that FEM modelling is based on idealizations concerning geometry, material properties, boundary conditions, interfaces and types of load application. Assumptions made in this field can affect the way the model predicts the distribution and severity of intracranial stresses and strains, which in turn affect the estimated injury patterns.

1.2 Current Research

Current helmet certification drop tests can only predict the protective capacity of a crash helmet in a limited way. The main limitations are the use of a rigid head form, because it does not model the dynamics of the real flexible human head correctly. Furthermore, only translational accelerations of the head form are measured, which is insufficient to predict injury. In relation to this the most commonly acknowledged and widely applied head injury criterion is the HIC (Head Injury Criterion), which is based on the assumption that the linear acceleration of the head is a valid indicator of head injury thresholds [2]. It is not capable of distinguishing between the different lesion mechanisms.

Currently at the Technische Universiteit Eindhoven a Ph.D. project is being carried out, titled "Modelling and specifications for an improved helmet design". Its objective is to improve the current test methodology, by introducing a physically more realistic head form. This head form will contain anatomical structures relevant in impact situations, such as a deformable skull and a brain model material.

A combined numerical experimental method will be used to determine relevant measured parameters for predicting the protective capacity of a crash helmet. Therefore numerical models of the head form and helmet will be developed. These models are partially validated against experimental data reported in literature; for additional validation we need to measure field parameters during a real drop test. These parameters will be obtained using a bi-plane X-ray setup, residing at the Technische Universiteit Eindhoven (see Figure 1.1). The images of the impact are recorded with two 15 inch image intensifiers, which makes the experimental drop test setup unique. The improvements to the dummy head form, as well as the determination of the relevant parameters in drop tests, will also be beneficial to the improvement of whole-body crash dummies.

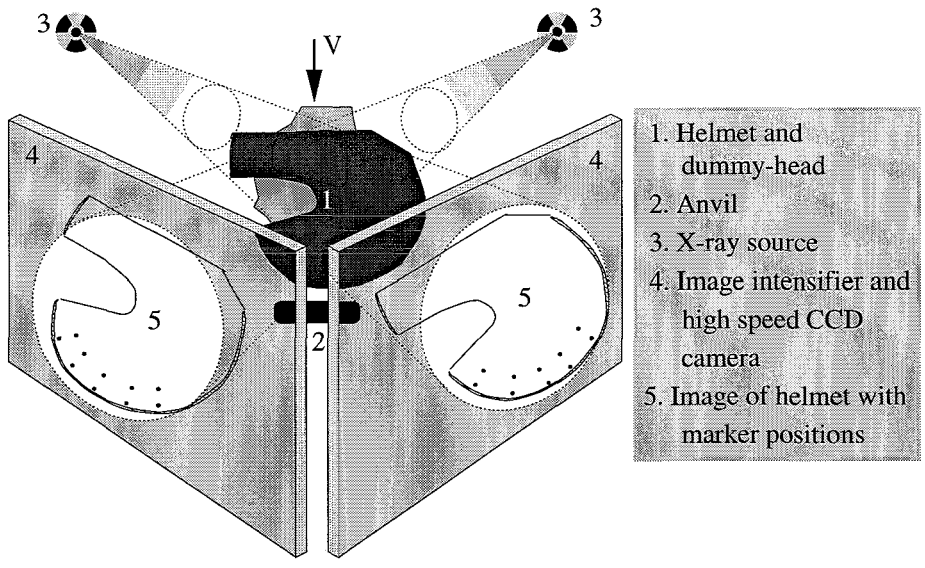

Figure 1.1: Bi-plane X-ray setup at the Technische Universiteit Eindhoven

In this thesis first a rigid head form will be developed according to the standard ECE-R22 regulations [6]. This head form will be used in standard helmet drop tests. Further a more realistic and biofidelic head form will be designed. Relevant anatomical structures such as the brain and the chin area will be represented. Relative kinematics between e.g. brain and skull then can be determined using neutral density markers placed in the brain model material and in the artificial skull. The physical model will be validated against available data from literature. Finally a numerical 3D FEM model will be developed and validated against the head form.
The improved guidelines relating to the head forms and the testing procedures will be formulated on the basis of the validation experiments with the head form.

Chapter 2

Head model properties

2.1 Introduction

To gain insight in the various properties of the standard head form (mechanical, geometrical, modal), some experiments will be carried out on the currently used head form. The standard head form is built according to specifications set in the ECE-R22 regulations [6], which prescribe the following characteristics:

- The head form shall be made of a metal with characteristics such that the head forms present no resonance frequency below 3000 Hz;
- The head form (with a circumference of 60 cm) has a mass of 5.6 $\pm$ 0.16 kg;
- The geometric properties of the head form must meet the shape and dimensions of a prescribed reference head form.

A standard dummy head form is supplied by the Crash Safety Research Centre of the TNO Road Vehicles Research Institute. The head form is made of aluminum and is supposed to meet the required specifications.

First in Section 2.2 a modal analysis will be carried out on this standard dummy head, in order to investigate its lowest resonance frequencies. Section 2.3 deals with the geometry of the dummy head model.

2.2 Modal analysis

It is to be expected that the lowest resonance frequencies of the standard dummy head are (well) above 3000 Hz, as required by the ECE-R22 regulations. When used in the high-speed bi-planar x-ray system, the aluminum head form will absorb nearly all radiation, and possible markers placed in an anatomical structure *inside* the head will not be visible. It therefore eventually will be necessary to replace the aluminum with another material, preferably with the same mechanical properties, but with a lower density. Polymers seem to be a good substitute material, because of their low density and good mechanical properties. In general their density is half of that of aluminium, see Table 2.1 below.

	Density ρ $[^{kg}/_{m^3}]$	*Young's Modulus* E $[^{N}/_{m^2}]$
aluminium	2700	$70 * 10^9$
polymers	1500	$3.5 * 10^9$

Table 2.1: Density and Young's modulus of aluminium and polymers

A rough estimate for the lowest resonance frequency ω of the head form can be made by substituting the material properties in Equation 2.1. This definition of ω is allowed for linear structures, potentially slightly damped. The stiffness k of the structure is rewritten, considering the head form a straight cylindrical beam, with a typical length l and thickness d.

$$\omega = \sqrt{\frac{k}{m}} \sim \sqrt{\frac{\frac{EI}{l^3}}{\rho V}} \sim \sqrt{\frac{\frac{Ed^4}{l^3}}{\rho d^2 l}} \sim \sqrt{\frac{Ed^2}{\rho l^4}} \tag{2.1}$$

where:

k = stiffness
m = mass
E = Young's modulus
I = momentum of area
ρ = density
V = material volume
l = characteristic material length
d = characteristic material thickness

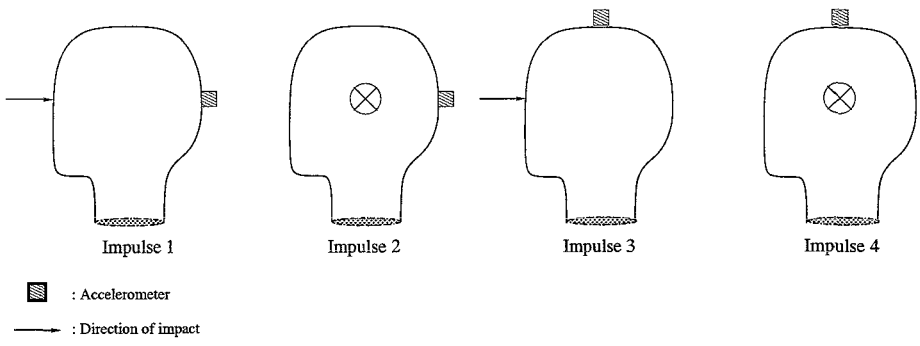

Figure 2.1: Position of measurements on the head form

According to Equation 2.1 the resonance frequency ω roughly will decrease by a factor 3. To compensate for this decrease the polymer head form wall thickness d can be increased.

2.2.1 Measurements

The head form is considered a slightly damped, linear structure. To determine the resonance frequencies, the head form will be supplied with an impulse, by hitting it with a hammer equipped with a force transducer. The frequency response is measured by an accelerometer connected to the head form. Both the input and output signals are sampled simultaneously and via a Fast Fourier Transformation the transfer function is computed by the software package Difa [7], showing the resonance frequencies of the structure. The position of the accelerometer on the structure and the direction of impact are chosen as shown in Figure 2.1.
Every measurement is repeated ten times to improve coherence. The computed transfer functions and their associated coherence figures are presented in Figure 2.2. Clearly the lowest resonance peak is situated near 6000 Hz. It should be noted that these results should be interpreted qualitatively only because of the amount of noise present. For an estimate of the order of magnitude of the lowest resonance frequency however the results are useful.

In conclusion, by increasing the head form wall thickness d (e.g. by a factor 2) the decrease of the lowest resonance frequencies (as a result of different material properties) can be compensated for. A polymer head form then will still meet the required specifications by ECE in the field of resonance.

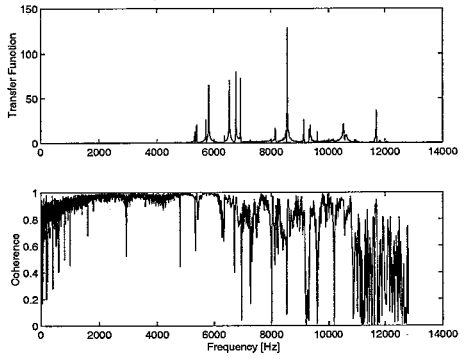

(a) Impulse 1

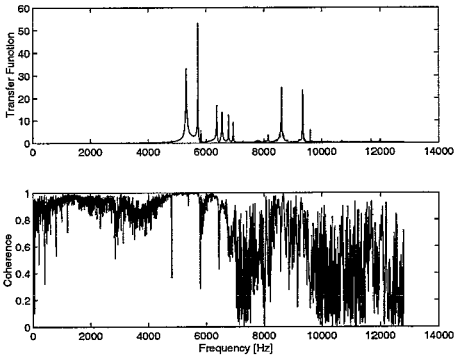

(b) Impulse 2

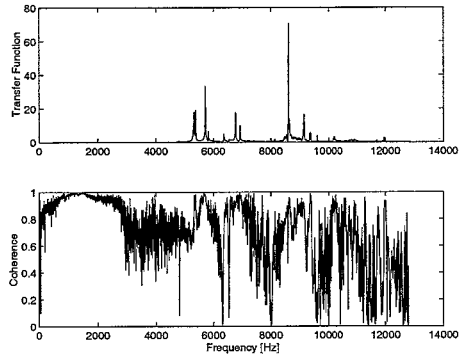

(c) Impulse 3

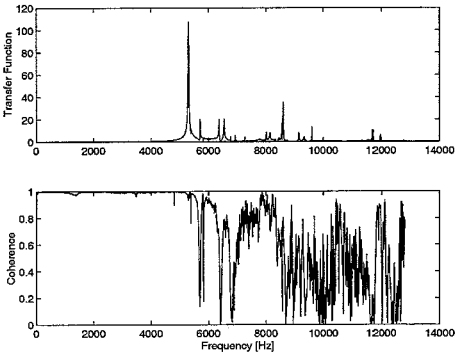

(d) Impulse 4

Figure 2.2: Head form transfer functions

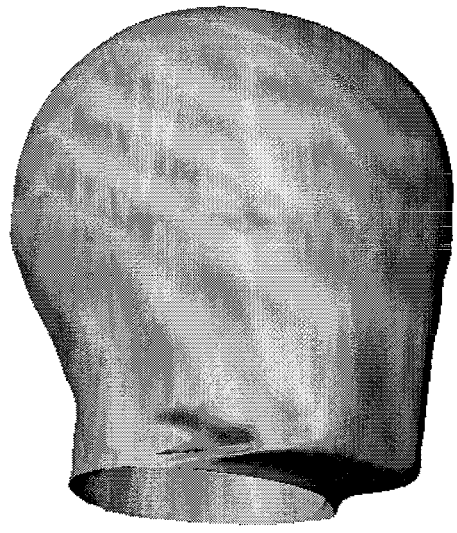

Figure 2.3: CAD/CAM prototype

2.3 Determination of the head geometry

The head form eventually will be built by a threedimensional milling machine. The milling process is controlled by a CNC-programme coming from a CAD/CAM software package; its input consists of geometrical data points of the standard head form, which are prescribed by the ECE-R22 regulations. These data points however are not suitable as input for a CAD/CAM programme, because of the lack of points in the chin and jaw area (see Figure 2.3). The CAD/CAM software fits splines through the data points and obviously problems arise in the mentioned areas. It therefore will be necessary to gather additional points, which is done by measuring the geometry of the existing dummy head.

2.3.1 Measurements

In order to obtain accurate head geometry data a TNO crash dummy head was measured using a 3-dimensional coordinate measuring device (Mitutoyo AE-122). A schematic overview of the device is given in Figure 2.4. The device consists of [8] a guide system that allows a spherical probe to be moved in three dimensions. The position of the probe is determined using optical

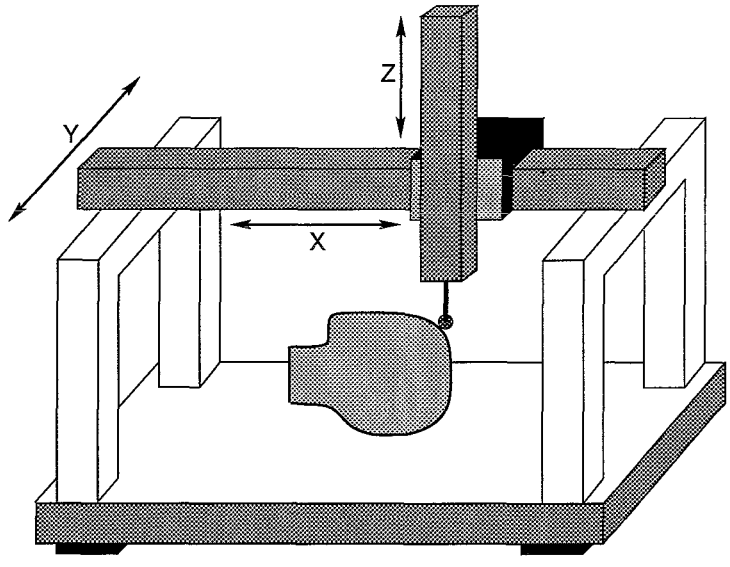

Figure 2.4: Mitutoyo 3-D measuring device

rulers. The ruler signals are transferred via a Mitutoyo MAG-1 measuring amplifier to a personal computer. Various software packages take care of transferring the data.

A typical measuring session consists of the following steps:

1. **Probe Calibration**
   Calibration of the probe, i.e. determination of the probe diameter, takes place by moving it towards a calibration sphere with a diameter of 25.4 mm (1 inch). From a set of measurements the properties of the probe are calculated by the Mitutoyo GEOPAK-3 software package (version 3.05).

2. **Definition of a (local) coordinate system**
   The use of a local coordinate system is necessary, for not all points can be reached with the probe if the head is fixed in one position. An adjustable fixation of the head was designed to overcome this problem. In order to determine the coordinate system, the probe is placed on certain known points on the object and the following three steps are carried out consecutively (see also Figure 2.5):

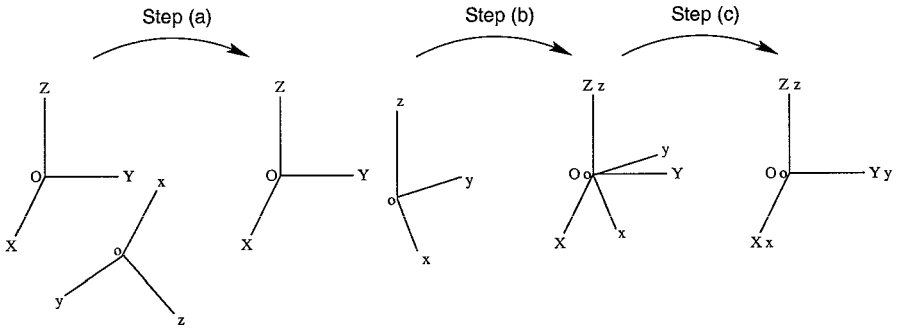

Figure 2.5: Steps for defining the local coordinate system

(a) *spatial aligning*
Three points in one plane perpendicular to the object x, y, or z-axis are indicated and the z-axis is aligned to the corresponding machine coordinate axis;

(b) *definition of the origin*
The object origin is joined with the machine coordinate system origin.

(c) *aligning of the axes*
The machine coordinate system is rotated over the axis perpendicular to the orthogonal plane so that all axes are aligned.

3. **Actual measurement**
The actual measurements are carried out with the Mitutoyo SCANPAK-3 software package (version 4.30). The probe is moved along the head's outer surface, while the software package registrates data points every 0.2 mm.

When the position of the head is changed all three steps are carried out again. In this way eventually four suitable data sets are collected and will be combined later on.

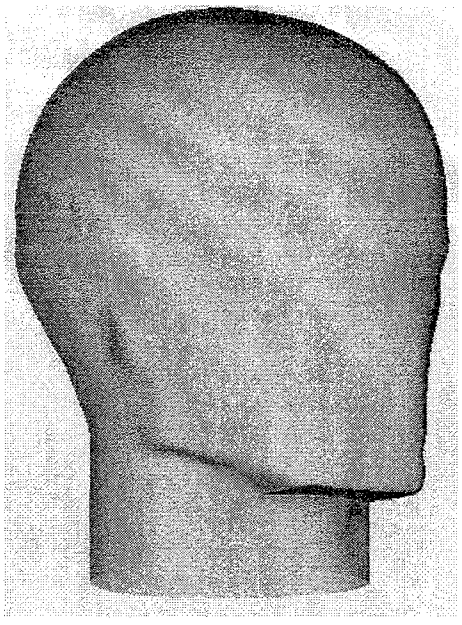

Figure 2.6: Improved CAD/CAM prototype

2.3.2 Data post processing

The stored coordinates are joined, to fill the complete geometry of the head form. This is done with the software package Altair HyperMesh v3.0. Samples of the points in the relevant areas (chin and jaw) are taken, to prevent an overflow of data. The prescribed data set is filled up with the samples and now a suitable input for the CAD/CAM software package MasterMill is ready. The result of the above described actions is shown in Figure 2.6. When compared to Figure 2.3 the improvements are obvious.
It is now possible to create a rigid head form, as a first step towards an improved, more biofidelic head form.

In the next chapter an overview is given of former research in the field of physical head modelling and relevant anatomical structures are investigated. The results will be used in developing an improved head form.

Chapter 3

Physical head modelling

Often investigations into head biomechanics involve the use of numerical (Finite Element) simulations. Numerical head models that are developed need to be validated in order to obtain a quality assessment of the calculated parameters. Therefore the numerical results must be compared with experimental results. It is not possible to perform in-vivo measurements of certain field parameters (such as stress and pressure) inside a biological structure under impact conditions, so alternative experiments have to be done. Experimental data from tests with animals and human cadavers often is used for the validation of the numerical results; these tests however have many experimental and ethical drawbacks. Also converting the results from animal experiments to actual human head behaviour introduces inaccuracies. The use of cadavers for validation purposes has the drawback of not knowing to what extent a cadaver shows the same behaviour as a human being under impact conditions [9]. Physical models should provide insight into the local brain response, but the inevitable differences between the head model and the real human head prevent the derivation of correct injury criteria. Because of the often well-defined physical model properties, experimental results may provide a first step in the validation of numerical models, or can be a starting point for parametric studies.

To date physical modelling of the human head mainly was emphasized on modelling (sub)structures of the head, such as the skull and brain [10], the brainstem and the cervical spine [11]. Other models only covered a specific field of research, such as modal behaviour of the head [12]. Little research yet is reported concerning the development of a physical total human head model.

Relevant research on physical head modelling is reported in section 3.1. In Section 3.2 relevant anatomical structures to be modelled in (motor cycle) head impact are discussed. Finally in Section 3.3 recommendations are given to improve the current physical head model.

3.1 Literature survey

Margulies [10] developed simple physical models of the head to investigate Diffuse Axonal Injury (DAI) in primates and humans. A silicone gel, as a brain model material, was poured into full and half cylinders, corresponding to mid-coronal cross-sections of the human head. To investigate their dynamical behaviour, the models were subjected to a prescribed rotation or translation and the resulting strains were derived from the motion of a grid layer painted onto a surface in the middle of the gel. The presence of a falx cerebri, represented by a polyurethane plate, clearly reduced deformation of the brain in comparison with a model without the falx cerebri. Regions with large shear strains in the model corresponded with regions in the human brain most often associated with DAI. Figure 3.1(a) shows the models, with (model A1 or B2) and without (model B1) a falx cerebri.
Similar work was done by Thibault *et al* [13], Margulies *et al.* [14] and Arbogast *et al.* [15], all using a Dow Corning Silicone Gel System as a model material for brain tissue. Arbogast *et al.* [15] are the only ones to justify the use of it, by presenting actual data on the materials's properties. Various other authors report of their work on developing a surrogate brain matter with material properties close to those of the human brain [16, 17, 18, 19, 20, 21]. Among other materials silicone gels with different ratios of polymer to catalyst were tested and the results are promising when compared to actual brain material properties.

Bilston et al. [11] examined the mechanical characteristics of the head and neck structure, with special emphasis on the spinal cord. Apart from (relaxation) experiments with human cadaver cervical and thoracic spinal cords also tests were conducted with an anatomically and mechanically accurate physical model (Figure 3.1(b)). A plastic reproduction of a human skull was sectioned sagitally, preserving the foramen magnum and atlanto-occipital articulation. With the use of polymer reproductions of the intervertebral disks and surrogate ligaments kinematic biofidelity during loading was preserved. The surrogate spinal cord was constructed in a nearly cylindrical mould, with a curvature at one end to represent the brainstem. The cylinder was divided longitudinally in two halves which both were filled with a

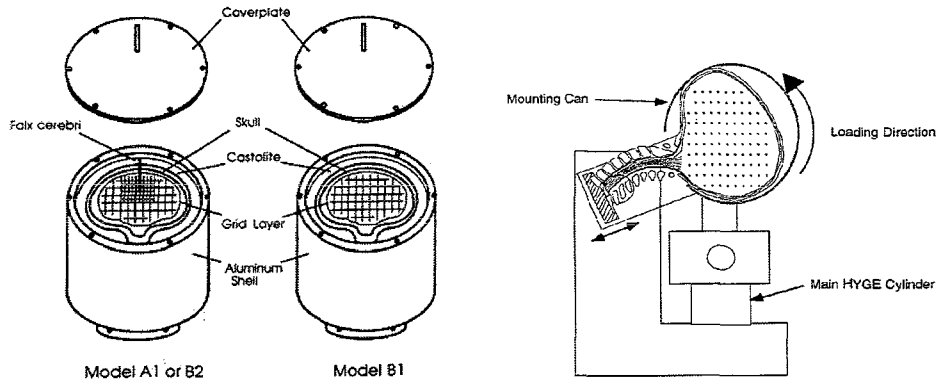

(a) Skull physical model [10]

(b) Head/neck physical model [11]

Figure 3.1: Physical models of brain, head and neck

brain surrogate material, a Sylgard silicone gel (Dow Corning). To visualize deformation, a grid of enamel dots was painted on the mid-sagittal plane surface of the cord/brainstem model and the brain model. Validation was accomplished by comparing the kinematic behaviour of the model with normal human kinematics.

Willinger et al. [12] concentrated on modal analysis of the human head. Research on lesion mechanisms leading to head trauma showed that the decoupling of the cerebral mass and the skull plays a fundamental role in the arising of lesions. Therefore a model called the *Bimass 150* was developed. It consists of two masses, one representing the brain and one representing the rest of the head, connected through a mechanical liaison such that the system's natural frequency is at 150 Hz (see Figure 3.2). Around this frequency the human head shows its first natural (resonance) frequency and decoupling of the human brain and skull occurs. The human head here is modelled as a multi-body system, in which relative motion is allowed for two rigid structures representing the skull and the brain. This is in contrast with the rigid body dummies recommended by European and North American standards for crash helmet performance tests. The *Bimass 150* dummy is said to enable detection of shear stresses and relative motion between skull and brain, which are important factors in the causing of head trauma. A distinction between translational and rotational shocks however cannot be

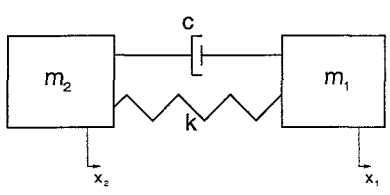

(a) Lumped parameter model

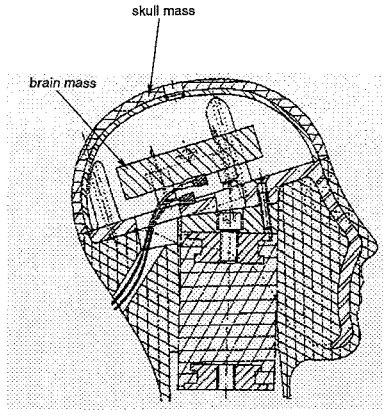

(b) Physical model schematic

Figure 3.2: Bimass 150 head model [12]

made. Apart from that only translational head motion in one impact direction is accounted for (as is the case with HIC), even though rotational accelerations are believed to be the cause of several head injuries. It was concluded that protecting the human head against impact forces is a matter of damping "intelligently", i.e. avoiding certain frequency ranges or certain temporal forms of the loading function.

The British Defence Evaluation and Research Agency (DERA) developed a full physical human head model, the DERAMan (Dynamic Event Response Analysis Man) [22]. This commercially available model is made of various polyurethane materials representing the brain, skull and skin of the human head. A lot of effort is made in the exact mimicking of the human head, whereas other research projects only model relevant anatomical structures. Detailed information on material properties and geometry is lacking. The model is said to be capable of measuring stress waves (both shear and compression waves) as well as socalled 'forces of motion', by the embedding of over 90 piezoelectric sensors and accelerometers. Processing of the data however still is a problem. Results and further research on injury mechanisms or tolerance levels is not available. The model has not been validated yet. This will be done by comparing the findings of tests with the model with clinical data from people with fatal head injuries.

The previously discussed models all are aimed at the mimicking of one particular structure or property of the head. In this project a more elaborated head model, containing various relevant substructures, will be modelled, both physical and numerical.

3.2 Relevant anatomical structures

Injuries to the head are predominantly located at the front side, with more than two thirds of skull fractures involving chin impact [3, 23]. The back of the head receives relative few injuries, merely because the back of the head often is not impacted. The head with the face region, especially the chin and forehead, is nearly always exposed to impact risks. Globally, 55% of the head injuries to motorcyclists are soft part injuries; skull fractures represent about 15%. Internal injuries such as commotio and contusio cerebri represent another 30% of the sustained head injuries [3].
From all the injuries sustained by helmet-wearing traffic participants, it is important to identify those head injuries that are relevant in impact situations.

3.2.1 Skull

In general skull bending is the cause of linear skull fracture. As a result of an impact the skull bends inwards at the site of the impact and bends outwards at some distance from the impact site. When the skull is deformed beyond its loading capacity, it fractures. Since bone is weaker in tension than in compression, cracks will appear at the skull's outer table in regions where the skull bends outwards, and on the inner table in regions where the skull bends inwards [24]. It is not intended to simulate skull fractures in the drop tests, but a deformable skull with mechanical properties close to those of the human skull contributes to a more realistic behaviour of the head model as a whole, which improves its biofidelity.

3.2.2 Chin

A high proportion of fatalities with head injuries sustained a fractured base of the skull. Almost always this was caused by a direct impact, through the chin guard of the helmet, to the facial skull and in turn through to the skull base [25]. The chin guard of the helmet therefore is an area of particular

	skull injuries	*focal brain injuries*	*diffuse brain injuries*
	vault fractures	epidural hematoma	mild concussion
	linear	subdural hematoma	classical cerebral concussion
	depressed	contusion	diffuse injury
	basilar fracture	intracerebral hematoma	shearing injury (DAI)
hospitalisation		50%	40%
deaths		2/3	1/3
disability		+	++

Table 3.1: Important types of head injury and their clinical relevance [26]

interest and thus the modelling of the chin in the head form is essential in providing a better understanding of the relevant injury mechanisms.

3.2.3 Brain

Intracranial injuries are subdivided into two categories: diffuse brain injury and focal brain injury, accounting for 40% and 50% of head injury patients admitted to hospitals, respectively.
Diffuse brain injuries are associated with widespread brain damage and range from mild concussion and to diffuse white matter shearing. They account for one third of head injury deaths.
Focal brain injuries cause brain dysfunction due to local brain damage and/or the presence of masses within the cranium, causing brain shift, herniation and possible brain stem compression. Focal brain injuries account for two thirds of all head injury deaths and always include anatomical damage. Physically modelling the brain may provide a better insight in the occurring injury mechanisms.

Table 3.1 indicates the relative importance of various types of head injury with respect to hospitalisation, fatal outcome and disability.

3.2.4 Falx and tentorium

The brain is covered by several membranes as illustrated in Figure 3.3. Among other membranes the *dura mater* covers the cerebral hemispheres and contains two layers; the outer *periosteal* layer and the inner *meningeal* layer. The periosteal layer is attached to the inner surface of the skull, whereas the meningeal layer forms three partitions between the hemispheres by means of a double-fold:

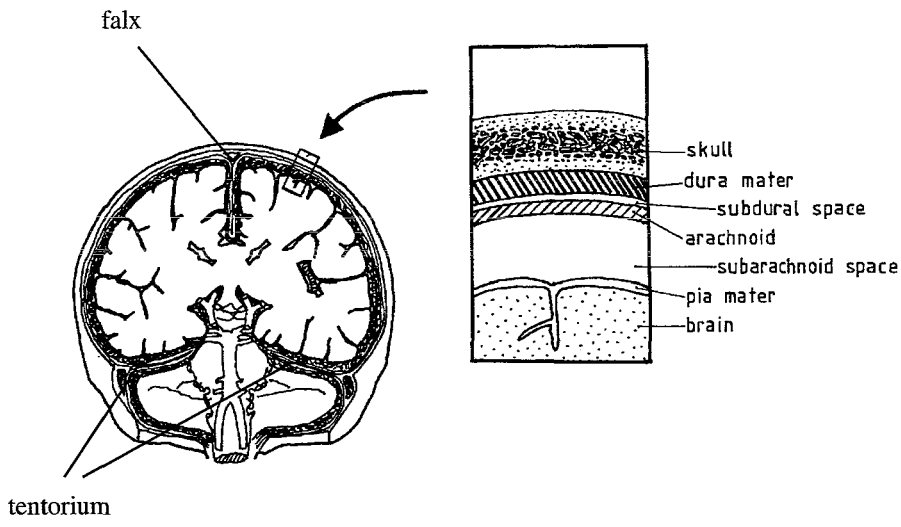

Figure 3.3: Position of falx cerebri and tentorium cerebelli

falx cerebri
the dural reflection separating the cerebral hemispheres;

falx cerebelli
the separation between the cerebellar hemispheres;

tentorium cerebelli
the separation between the cerebral hemispheres and the cerebellum.

Because of their special structure the falx and tentorium are much stiffer than the surrounding tissue. They hinder the relative movement, which locally leads to large deformations at the contact interfaces between brain and falx and/or tentorium, which is thought to be the main cause of contusions [27].

3.2.5 Scalp

The outer skin layer surrounding the skull is called the scalp. Injuries to the scalp, although quite common in impact situations, are considered to be of minor importance because of their low clinical relevance. This includes external structures such as the ears and the nose, as well as the eyes, also because they are well enough protected when wearing a crash helmet.

A physical model effectively simulating head impact on motorcyclists should be able to account for the possible injuries to the structures mentioned above.

3.3 Development of an improved head form

The currently used head forms often are solely supplied with (threedimensional) accelerometers, measuring the translational acceleration of the head's center of gravity during impact. Moreover, the head is considered a rigid body (no anatomical details are modelled) and no information in terms of stresses, strains or relative skull/brain displacement is obtained. By implementing relevant anatomical structures and measuring both translational and rotational accelerations, more information can be gathered on the head's behaviour under impact conditions.

According to the study in Section 3.2 relevant structures to be modelled are:

- a deformable *skull*, including the *chin*, as it will contribute to a more realistic behaviour of the head model as a whole;
- the *brain*, including a *falx cerebri*, as brain injuries account for a substantial part of head injury with fatal outcome. The falx influences the brain's behaviour and therefore should be modelled as well.

3.3.1 Skull

- *material*

A skull model material should approximate the human skull mechanical behaviour, in terms of Young's modulus and tensile strength. Fiber-reinforced composite materials seem to meet these requirements. An overview of both the human skull properties and properties of skull model materials are listed in Table 3.3.1. Shown are averaged data taken from literature.
Because relevant skull impact predominantly takes place in the upper half of the human head, and also considering the brain model chosen in Section 3.3.2, this particular part of the skull (the *neurocranium*) will be modelled apart from the rest of the skull. The upper part of the physical head will be removed and replaced by a fiber reinforced composite part, filled with a brain model material. The rest of the skull will be modelled with another material, *polyacetal* (PolyOxyMethylene, POM). Its properties are also displayed in Table 3.2 and will be discussed further in Chapter 4.

	Human skull	Composites	POM
Material properties			
Density ρ $[^{kg}/_{m^3}]$	$1.41{\cdot}10^3$	$1.3\text{-}2.3{\cdot}10^3$	$1.41{\cdot}10^3$
Mechanical properties			
Young's Modulus E $[^{N}/_{m^2}]$	$6.5{\cdot}10^9$	$6\text{-}50{\cdot}10^9$	$3{\cdot}10^9$
Poisson's ratio ν [–]	0.2	variable	0.3

Table 3.2: Properties of human skull and skull model materials [9, 19, 28]

- *production method*

The skull geometry is obtained from the CAD/CAM data file, as gathered in Section 2.3 of this report. A threedimensional CNC-operated milling machine finally produces the physical head form. The inner skull surface and the outer brain surface must coincide with each other, to avoid inhomogeneities that may disturb the mechanical behaviour. This is not the case in the real human head, but it will prevent some of the numerical problems later on. In the next section the brain geometry will be discussed further.

- *experimental analysis*

Deformations of the skull can be measured by placing markers on the inner and/or outer surface of the physical skull model. High speed cameras will record the motion of the markers and relevant parameters (such as strains) can be determined. Depending on the used material model, also stresses can be calculated.

3.3.2 Brain

- *material*

The constitutive properties of the human brain in terms of Young's modulus E, Poisson's ratio ν, and density ρ are presented in Table 3.3. Various brain model materials have been investigated at the Technische Universiteit Eindhoven by Brands *et al.* [21]. A silicone gel system offered promising results in mimicking the dynamical behaviour of brain tissue and will be applied in the improved head form. More information on the model's material and mechanical properties also is shown in Table 3.3. Further elaboration on this matter is available in Chapter 4. It should be noted that usually the properties of (time-dependent) visco-elastic materials are given in terms of dynamic modulus and phase angle. When converting these data to an elastic modulus E, the time-dependence of the material moel is disabled.

		Human brain	Silicone gel system
Material properties			
Density ρ	$[^{kg}/_{m^3}]$	$1.04 \cdot 10^3$	$0.998 \cdot 10^3$
Mechanical properties			
Young's Modulus E	$[^{N}/_{m^2}]$	$1.00 \cdot 10^6$	$\sim 1 \cdot 10^6$
Poisson's ratio ν	$[-]$	0.48-0.5	0.4996

Table 3.3: Properties of human brain and brain model materials [9, 21]

- *production method*

The development of the physical and numerical brain model material should be coupled. When developing the numerical model, the physical realisation should be taken into consideration as well. In this case the main limitations derive from the physical brain model, as it is very difficult to physically model detailled and thus complex structures. A literature survey revealed a numerical brain model suggested by Bandak *et al.* [29]. This model originally was constructed by DiMasi *et al.* [30] and modified by Bandak *et al.* later on. The model is depicted in Figure 3.4. It consists of a dura mater that includes the falx cerebri. The tentorium and falx cerebelli are not modelled explicitely. The model does not account for the details of the cerebellum, the midbrain, and the brain stem. Though further arguments explaining the choice of this particular configuration are lacking, the model is widely accepted and used in numerical simulations. Merely because of its relatively simple geometry, the *Bandak*-model relatively easy can be applied in the improved head form, both experimental and numerical. As a first approach the falx cerebri will not yet be modelled.

- *experimental analysis*

Deformations in the brain are more difficult to measure than deformations in e.g. the skull, as the presence of markers in the brain model material can alter its dynamical behaviour. On top of that the markers can damage the material and move *through* the material with the result that they no longer move with the brain. Therefore markers with an identical density or a density close to that of the brain model material have to be used. Experiments with such markers have been done previously by Hardy *et al.* [31, 32]. They used Neutral Density Targets to measure deformation patterns in the human brain. A high-speed biplanar X-ray setup enabled the determination

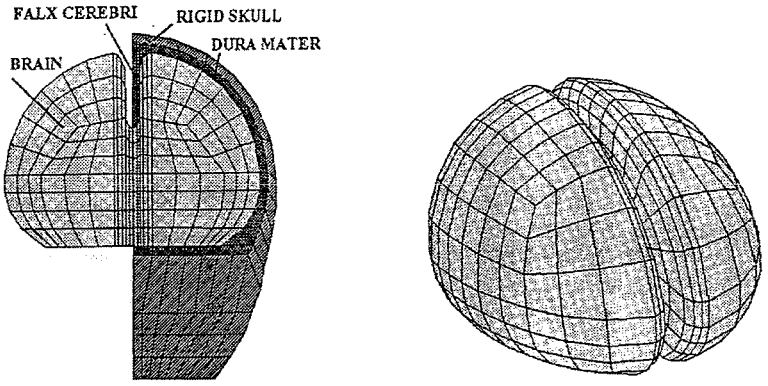

(a) Midcoronal view of the *Bandak*-model

(b) Three dimensional view of the brain alone

Figure 3.4: The *Bandak*-model [29]

of the strain in a relatively small volume of brain. The targets are made from thin-walled polystyrene tubing. They are 2.34 mm-diameter cylinders, 3.90 mm long. Stainless steel balls of 1.6 mm are fixed via cyanoacrylate in the center of the target tubing. The ends of the tubes are capped with thin sheets of styrene. The density of the targets is at or below 1.05 $^{g}/_{ml}$, which comes close to value of 1.04 $^{g}/_{ml}$ used by Claessens [9] for brain tissue in numerical simulations of head impact. The targets cannot be placed too close to each other as there may be interference or overlap in the bi-planar images. To avoid target confusion the amount of markers that can be placed into the brain is limited; quantitative remarks however are lacking.

Chapter 4

Numerical Head Modelling

In Chapter 3 various recommendations have been formulated to improve the standard head form. This chapter mainly concerns the numerical modelling of both the standard physical head form (Section 4.1) and the improved head form (Section 4.2). Section 4.3 deals with a numerical simulation of head impact.
The used software package for Finite Element Modelling is MADYMO 3D version 5.4. Preprocessing was done by the Altair HyperMesh version 3.1 software package.

4.1 Solid Head Form

In this section the standard physical head form will be modelled numerically. Consecutively the generation of the mesh, the material properties and the dynamical properties of the model are dealt with.

4.1.1 Mesh Generation

Mesh generation was based on the head form geometry as prescribed by the ECE-R22 regulations [6]. Starting position is the mesh as earlier developed by Brands *et al.* [21] (see Figure 4.2). In this particular case the head form was considered rigid and had been modelled using 52 SHELL4 shell elements[1], containing four nodes each.

In the previous chapter it became clear that, in order to improve the standard head form, the head should be modelled as a deformable structure.

[1] More information on element types is available in appendix A

This demand no longer allows the use of shell elements, that solely possess in-plane and bending stiffness. The model therefore will be built out of SOLID1 or SOLID8 brick elements[1], with tensile, compression and shear stiffness. From a computational point of view the choice of hexahedral (brick) elements is cheaper than for example tetrahedral elements. In this section the mesh generation of the solid head form will be discussed.

HyperMesh is able to generate a solid mesh between two surfaces, an inner and an outer surface, formed by shell elements. One surface of shell elements is available, i.e. the numerical model developed by Brands *et al.* [21]. This is considered the outer surface. When constructing the inner surface, the following requirements must be met:

- The number of shell elements of inner and outer surface are equal;
- The topology of both surfaces must be equal;
- The inner surface geometry must be chosen as simple as possible, for the volume enclosed by the inner surface itself also must be filled with solid elements.

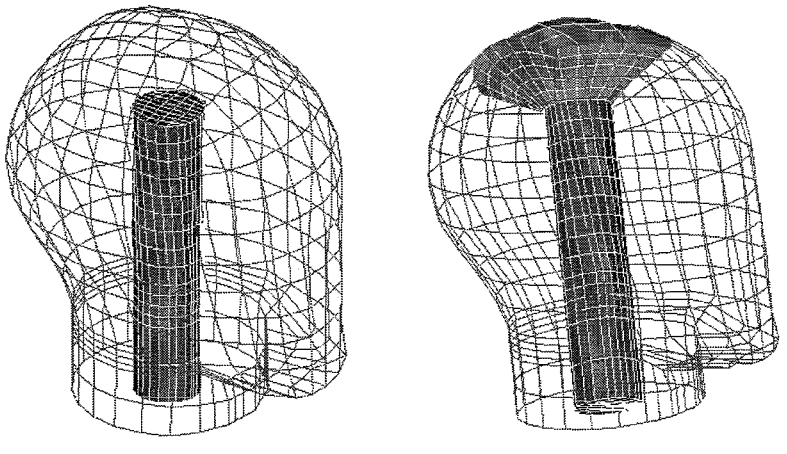

(a) Inner and outer surface of the numerical head model

(b) Solid elements between neurocranium and cylinder top

Figure 4.1: Mesh generation

The mesh generation process is illustrated in the Figures 4.1 and 4.2. The inner surface is chosen a cylinder with a surface of 430 shell elements, which corresponds to the number of elements of the outer surface (Fig. 4.1a). Its upper surface consists of 40 elements, corresponding to the upper part of the outer surface (the neurocranium) that will be projected onto it (Fig. 4.1b).

First the outer mesh surface is edited. Two element layers in the chin area are subdivided into a total of four layers to equalize the inner and outer mesh surface and to enable the formation of elements between these surfaces. Consecutively the inner cylinder is filled with solid elements, and SOLID1 elements are formed between the two surfaces (Fig. 4.2).

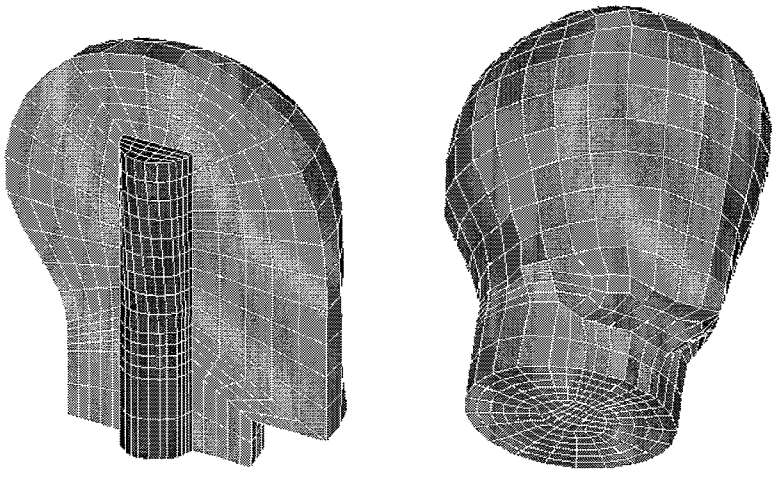

(a) (b)

Figure 4.2: Final head model consisting of solid elements

Finally all shell elements are removed; the solid head model now consists of 2750 solid elements, with a total of 3084 nodes. As a first step, the size of the elements is chosen in accordance with the element size of the existing outer shell layer. Especially for linear elements, large gradients of field parameters over the elements are better estimated using more and smaller elements. In general a less refined mesh tends to show a more stiff

behaviour of the numerical model, but is cheaper in terms of computional costs. Further research on the effects of mesh refinement is recommended in order to develop an optimized mesh.

4.1.2 Material Properties

The numerical head form is given the material properies of the physical head form, made of *polyacetal (POM)* as described in subsection 3.3.1. POM offers the advantages of desirable material properties and good machining properties. Relevant properties are given in Table 3.2. In a first approach the material model is assumed linear elastic and isotropic to describe the constitutive behaviour of POM.

4.1.3 Dynamical Properties

Simulation in MADYMO yields information on the model's mass, center of gravity and principal moments of inertia. These parameters play an important role in the tuning of the numerical head model later on, as they are related to the biofidelity of the model. Values for mass and moments of inertia of the numerical head model are given in Table 4.1.

To accurately model the physical head's features, also the accelerometer and three angular rate sensors are represented in the numerical model. The sensors are modelled as lumped masses attached to a single node. With a combined mass of approximately 200 $[gr]$ no significant influence on the principal moments of inertia was observed. By removing material in the neck part and the inside of the head its inertial properties will be altered and tuned to the inertial properties of a standard head form, the HYBRID-III. The HYBRID-III dummy head currently is used for standardizing safety systems and its properties are similar to the human head inertial properties [33]. Inertial properties of the tuned head model and the HYBRID-III also are given in Table 4.1.

		Solid head	*Tuned head*	*Hybrid III head*
Mass $[kg]$		6.65	5.65	5.61
Moments of Inertia	I_{xx}	$3.396{\cdot}10^{-2}$	$2.762{\cdot}10^{-2}$	$1.590{\cdot}10^{-2}$
$[kg \cdot m^2]$	I_{yy}	$4.026{\cdot}10^{-2}$	$3.399{\cdot}10^{-2}$	$2.400{\cdot}10^{-2}$
	I_{zz}	$2.414{\cdot}10^{-2}$	$2.353{\cdot}10^{-2}$	$2.200{\cdot}10^{-2}$

Table 4.1: Mass and moments of inertia of the numerical head models

Figure 4.3 shows the tuned head model. It should be noted that the elements are removed in a cylindrical shape inside the head. As already mentioned the development of the physical and numerical head form is coupled. In this way the removing of material inside the physical head form, necessary to place the senors, is facilitated.

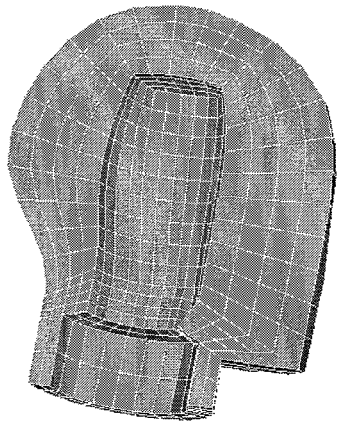

Figure 4.3: Mid-sagittal cross-section of the tuned head model

The relative large difference in moments of inertia between the tuned head model and the HYBRID-III dummy model (+80%, +42% and +3% for I_{xx},I_{yy} and I_{zz} respectively) can be explained by assuming the HYBRID-III dummy head is a standard 50%-tile head form, which is smaller and has a lower mass than the head form used in this project. This may lead to the observed higher values for the moments of inertia. Scaling of these data is complex, as it is difficult to determine a correct scaling factor.

To facilitate placing of the sensors in the physical head form, a module equipped with sensors will be constructed. This module has a cylindrical shape, corresponding to the inner surface of the tuned numerical head model. It contains three angular rate sensors and one triaxial accelerometer placed near the model's center of gravity, as prescribed by the ECE-R22 regulation [6].

4.2 Improved Head Form

In this section the numerical head form developed in the previous section will be improved by introducing anatomically relevant structures.

4.2.1 Modelled substructures

To improve the solid head form various substructures will be modelled to increase biofidelity. These substructures are the brain and the skull, including the neurocranium. In the first instance the falx cerebrum will not be modelled because of the complicated physical and, to a lesser extent, numerical modelling.

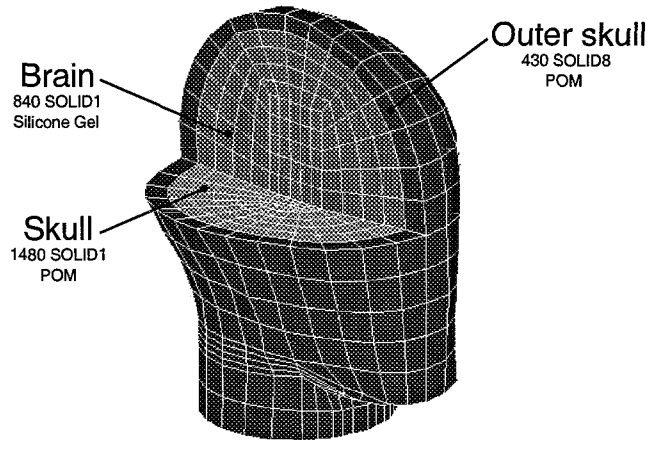

Figure 4.4: Numerical model of the improved head form with its different substructures and elements

4.2.2 Mesh Generation

The mesh of the head form developed in Section 4.1 is used as basis for the improved head form. In the outer element layer of the head the SOLID1 elements are replaced with SOLID8 elements (using eight integration points), that are able to handle bending of the outer skull layer, in particular the neurocranium.

The brain mesh is determined on the basis of the Bandak brain model presented in Section 3.3 (see Figure 3.4), yet no falx cerebrum is modelled. Figure 4.4 shows the improved head form with its different substructures, elements and number of elements.

4.2.3 Material Properties

The model material for the skull including the outer element layer is POM, as was the case in the previous section.

The brain model material is the Sylgard silicone gel system as discussed in Subsection 3.3.2. The material in a first approach is considered homogeneous, linear elastic and isotropic. Its relevant properties are given in Table 3.2.

4.2.4 Dynamical Properties

Again a simulation with MADYMO is carried out and the model's mass and moments of inertia are yielded. Parameter values are given in Table 4.2.

To enable the use of the sensor module as described in Subsection 4.1.3 the improved head form's internal geometry will be adapted and moreover it will be tuned to the HYBRID-III dummy. Results are given also in Table 4.2.

		Improved head	*Tuned improved head*	*Hybrid III head*
Mass	$[kg]$	5.99	5.26	5.61
I_{xx}	$[kg \cdot m^2]$	$3.115 \cdot 10^{-2}$	$2.543 \cdot 10^{-2}$	$1.590 \cdot 10^{-2}$
I_{yy}	$[kg \cdot m^2]$	$3.707 \cdot 10^{-2}$	$3.127 \cdot 10^{-2}$	$2.400 \cdot 10^{-2}$
I_{zz}	$[kg \cdot m^2]$	$2.227 \cdot 10^{-2}$	$2.163 \cdot 10^{-2}$	$2.200 \cdot 10^{-2}$

Table 4.2: Mass and moments of inertia of the improved head models

It should be noted that the module with sensors is not yet included in the tuned improved head, accounting for the lower mass. Qualitative remarks on the moments of inertia of the numerical improved head model cannot be made yet. They have to be compared to experimental data from the physical improved head form.

4.3 Simulation of Head Impact

The numerical improved head model is given an initial velocity of 7.0 $[^{m}/_{s}]$ to simulate the falling speed in the experimental setup. Impact is simulated by subjecting the outer skull layer to a typical (prescribed) acceleration field for a period of 15 $[ms]$. The outer skull layer thus is considered rigid.
Deformation patterns now can be obtained. Appendix B shows the Von Mises stresses in the numerical improved head model at various time steps. Maximum stresses of $1.7{\cdot}10^{5}$ $[^{N}/_{m^2}]$ seem to be located at the front side of the neurocranium. Qualitative conclusions however cannot be drawn yet, for the model has to be validated first. If further extended, numerical simulations will enable the analysis of local field parameters and give insight to possible injury mechanisms.

Chapter 5

Conclusions and recommendations

The project "Modelling and specifications for an improved helmet design", among other things, involves the development of an improved, more biofidelic dummy head form. This head form should give more insight in possible injury mechanisms that take place in the human head during impact loads. Insight in these mechanisms eventually will contribute to an improved helmet design.

5.1 Conclusions

- The ECE-R22 regulation does not sufficiently prescribe the head form's geometry; supplementary data is necessary;
- Relevant anatomical structures to be modelled in head impact on motorcyclists are the *skull*, the *brain*, the *chin* and the *falx cerebrum*.

The improvement of the head form developed in this project, compared to the standard (rigid) head form used in drop tests, is twofold:

- Relevant anatomical substructures are modelled, which improves biofidelity and enables research on local injury mechanisms;
- Providing the head form with an extra set of three angular rate sensors (besides the threedimensional accelerometer) and suitable markers in the various structures, yields information on field parameters possibly correlated to injuries.

The numerical simulations that are carried out are not yet suitable for profound analysis.

- If further extended, numerical simulations will enable the analysis of local field parameters and give insight to possible injury mechanisms.

With regard to the standard helmet certification test the following conclusion can be drawn:

- The current ECE-R22 regulation on head forms to be used in drop tests, is susceptible to structural improvements in the field of biofidelity.

5.2 Recommendations regarding future research

Future research should contribute to the ultimate goal of this project: the development of a fully validated, physically more realistic head form, representing all of the relevant anatomical structures. Therefore the following recommendations can be made:

physical head form

- A modal analysis should be carried out on the improved physical head form, in order to investigate its (lowest) resonance frequencies;
- The moments of inertia and center of gravity of the physical head must be determined and compared with the numerical results. Possibly the results must be tuned to each other;
- Drop tests with the standard head form and the improved head form will provide a great deal of insight in relevant field parameters.

numerical head form

- The influence of mesh refinement on the dynamical behaviour of the numerical model must me further investigated;
- The constitutive behaviour of the various model materials must be extended (e.g. linear elastic *vs.* (linear) viscoelastic, isotropic *vs.* anisotropic);
- Automatization of the tuning process will produce an optimized mesh and will save time;

- Numerical simulations must be extended in order to enable quantitative remarks on relevant field parameters.

Obviously the development of an improved head form is a combined action of physical and numerical research. For both disciplines yields:

physcial and numerical head form

- The head form as a whole must be further developed. Representation of extra substructures, such as *falx* and/or *tentorium* and the installing of a load sensor in the chin area are recommended;
- The numerical head form must be validated against experiments with the physical head model;
- In its turn the physical head has to be evaluated by means of results from literature.

Bibliography

[1] Centraal Bureau voor de Statistiek (1999) Aantal verkeersdoden in 1998 fors gedaald, *Persbericht Centraal Bureau voor de Statistiek CBS*, Voorburg/Heerlen, The Netherlands

[2] Wismans, J.S.H.M., Janssen, E.G., Beusenberg, M., Koppens, W.P., Lupker, H.A. (1994) *Injury Biomechanics*, course notes on lecture series, Eindhoven University of Technology, the Netherlands

[3] Otte, D., Jessl, P., Suren, E.G. (1984) Impact points and resultant injuries to the head of motorcyclists involved in accidents, with and without crash helmets, *1984 International IRCOBI Conference on the Biomechanics of Impacts*, Delft, The Netherlands

[4] Blokspoel, A. (1989) De verkeersonveiligheid in 1988, *Report R-89-34*, Institute for Road Safety Research SWOV, The Netherlands

[5] Beusenberg, M.C., Happee, R. (1993) An experimental evaluation of crash helmet design and effectiveness in standard impact tests, *1993 International IRCOBI Conference on the Biomechanics of Impacts*, Eindhoven, The Netherlands

[6] United Nations (1994) Regulation no. 22: Uniform provisions concerning the approval of protective helmets and of their visors for drivers and passengers of motor cycles and mopeds, *Agreement concerning the adoption of uniform conditions of approval and reciprocal recognition of approval for motor vehicle equipment and parts*, Geneva, Switserland; Including 04 series of amendments

[7] Difa Measuring Systems (1994-1995) *User manual FA 100 Fourier Analyzer*, Breda, The Netherlands

[8] Brands, D.W.A. (1996) Development and validation of a finite element method of a motorcycle helmet, *(internal) WFW-report 96.137*, Master's Thesis, Eindhoven University of Technology, The Netherlands

[9] Claessens, M.H.A. (1997) Finite element modeling of the human head under impact conditions, *Ph.D. Dissertation*, Eindhoven University of Technology, The Netherlands

[10] Margulies, S.S. (1987) Biomechanics of traumatic coma in the primate, *Ph.D. Dissertation*, University of Pennsylvania, Philadelphia, U.S.A.

[11] Bilston, L.E., Meaney, D.F., Thibault, L.E. (1993) The development of a physical model to measure strain in a surrogate spinal cord during hyperflexion and hypertension, *1993 International IRCOBI conference on the biomechanics of impacts*, Eindhoven, The Netherlands

[12] Willinger, R., Kopp, C.M., Ramet, M., Bouquet, R., Caire, Y. (1993) Proposition of a new dummy head: the Bimass 150 principle, *1993 International IRCOBI conference on the biomechanics of impacts*, Eindhoven, The Netherlands

[13] Thibault, L.E., Bianchi, A., Galbraith, J., Gennarelli, T.A. (1982) Analysis of the strains induced in physical models of the baboon brain undergoing intertial loading, *Proceedings of the 35^{th} Annual Conference on Biomechanics of Impact*, Dublin

[14] Margulies, S.S., Thibault, L.E., Gennarellis, T.A. (1985) Physical models of head injury, *Proceedings of the 38^{th} Annual Conference on Engineering in Medicine and Biology*, Chicago, Illinois

[15] Arbogast, K.B., Thibault, K.L., Pinheiro, B.S., Winey, K.I., Margulies, S.S. (1997) A high frequency shear device for testing soft biological tissues, *J. Biomechanics*, volume 30, no. 7, pp757-759

[16] Margulies, S.S., Thibault, L.E., Gennarelli, T.A. (1990) Physical model simulations of brain injury in the primate, *J. Biomechanics*, volume 23, no. 8, pp823-836

[17] Meaney, D.F., Ross, D.T., Winkelstein, B.A., Brasko, J., Goldstein, D., Bilston, L.B., Thibault, L.E., Gennarelli, T.A. (1994) Modification of the cortical impact model to produce axonal injury in the rat cerebral cortex, *Journal of Neurotrauma*, volume 11, no. 5, pp599-612

[18] Viano, D., Aldman, B., Pape, K., van Hoof, J., von Holst, H. (1997) Brain kinematics in physical model tests with translational and rotational acceleration, *Int. J. Crashworthiness*, volume 2, no. 2, pp191-205

[19] Meulman, J.H. (1996) An experimental investigation to the constitutive behaviour of brain tissue, *(internal) WFW-report 96.059*, Master's Thesis, Eindhoven University of Technology, The Netherlands

[20] Plasmans, C.J.P. (1998) The dynamical behaviour of a model material for brain tissue, *(internal) WFW-report 98.021*, Eindhoven University of Technology, The Netherlands

[21] Brands, D.W.A., Bovendeerd, P.H.M., Peters, G.W.M., Wismans, J.S.H.M., Paas, M.H.J.W., van Bree, J.L.M.J. (1999) Comparison of the dynamic behaviour of brain tissue and two model materials *Proceedings 43^{rd} Stapp Car Crash Conference*

[22] Moore, P. (1997) A very smart dummy, *New Scientist July 5^{th} 1997*, Volume 154, No. 2089, IPC Magazines Limited

[23] Otte, D. (1991) Technical demands on safety in the design of crash helmets for biomechanical analysis of real accident situations, *35^{th} Stapp Car Crash Conference*, pp335-339

[24] Van den Bosch, H.L.A. (1998) Modelling and specifications for an improved helmet design - A literature review, *(internal) WFW-report 98.030*, Eindhoven University of Technology, The Netherlands

[25] Hurt, H.H. jr., et al. (1986) Epidemiology of head and neck injuries in motorcycle fatalities. In *Mechanisms of head and spine trauma by Sances, Thomas, Ewing, Larson and Unterharnscheidt*, Aloray

[26] Chapon, A., Verriest, J.P., Dedoyan, J., Trauchessec, R., Artru, R. (1983) Research on brain vulnerability from real accidents, *ISO\TC 22\Sc12\WG6-Document N139*

[27] Gennarelli, T.A. (1985) The state of the art of head injury biomechanics - A review, *29^{th} Conference of the association for the advancement of automotive medicine*, pp47-63

[28] McElhaney, J.H., Fogle, J.L., Melvin, J.W., Haynes, R.R., Roberts, V.L., Alem, N.M. (1970) Mechanical properties of cranial bone, *Journal of Biomechanics*, volume 3, pp495-511

[29] Bandak, F.A., Eppinger, R.H. (1994) A Three-Dimensional Finite Element Analysis of the Human Brain Under Combined Rotational and Translational Accelerations, *Proceedings 39th Stapp Car Crash Conference, SAE paper 942215*, pp145-163

[30] DiMasi, R., Eppinger, R.H., Gabler, H.C., Marcus, J. (1991) Simulated Head Impact with Upper Interior Structures Using Rigid and Anatomic Brain Models, *Auto and Traffic Safety D.S. Strombotne (ed. National Highway Traffic Safety Publication)*, Volume 1, No. 1

[31] Hardy, W.N., Foster, C.D., Tashman, S., King, A.I. (1997) Current findings on the kinematics of brain injury, *Symposium preproceedings Centre for Disease Control and Prevention (CDC)*, Atlanta, U.S.A.

[32] Hardy, W.N., Foster, C.D., King, A.I., Tashman, S. (1998) Update on the study of head-injury kinematics, *Symposium Proceedings Centre for Disease Control and Prevention (CDC)*, Atlanta, U.S.A.

[33] Willinger, R., Guimberteau, T. (1998) Development of a new headform -the Bimass 150 Dummy Head-, *Final report Study Contract European Community COST Transport 327*, Universite Louis Pasteur, Strasbourg, France

Appendix A

Element types

SHELL4

The SHELL4 element is a plane, constant stress quadrilateral element, with in-plane and bending stiffness and a lumped mass distribution over the nodes. It connects four nodes, each having five local degrees of freedom: three translational and two rotational; the element has no rotational degree of freedom perpendicular to its plane. Instead of complete integration it uses *reduced* integration with just one integration point.

SOLID1

The SOLID1 element is a brick element with tensile, compression and shear stiffness. It connects eight nodes, each with three translational degrees of freedom. The stress and strain components are defined with respect to the inertial coordinate system. Due to the reduced integration used, the SOLID1 element has the drawback of hourglass modes. It therefore uses a stabilisation method to prevent hourglass deformation, as does the SHELL4 element.

SOLID8

The SOLID8 element is the same as the SOLID1 element, only complete integration is used. Due to this full integration the SOLID8 element uses more CPU time compared to SOLID1, but has the benefit of the absence of hourglass modes.

Appendix B

Numerical simulation results

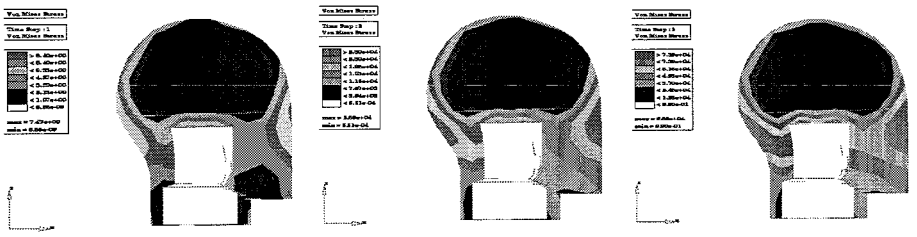

(a) t=0.001 (b) t=0.002 (c) t=0.003

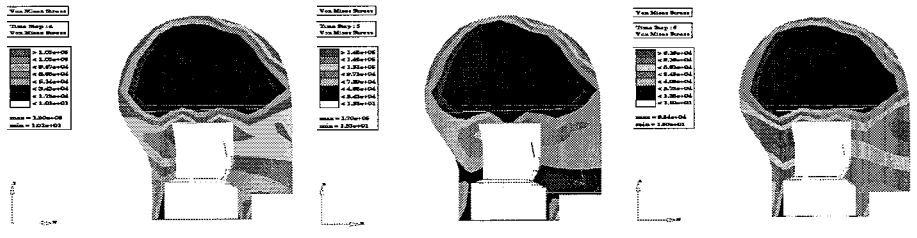

(d) t=0.004 (e) t=0.005 (f) t=0.006

Figure B.1: Von Mises Stresses in the numerical head model

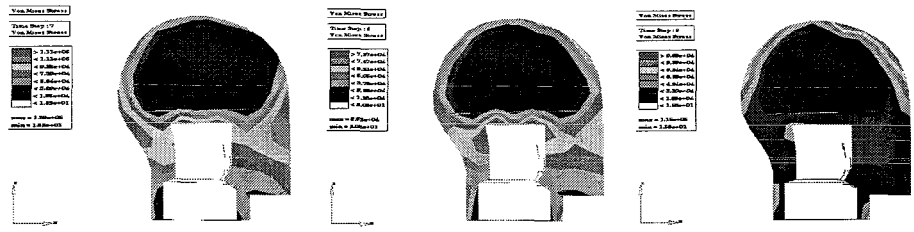

(a) t=0.007 (b) t=0.008 (c) t=0.009

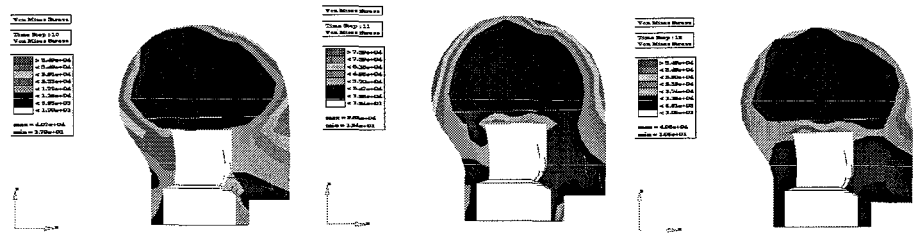

(d) t=0.010 (e) t=0.011 (f) t=0.012

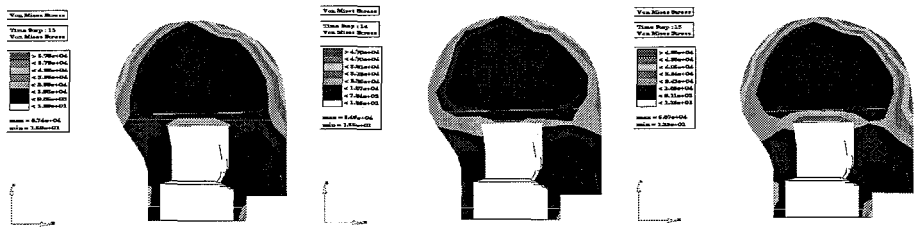

(g) t=0.013 (h) t=0.014 (i) t=0.015

Figure B.2: Von Mises Stresses in the numerical head model

Abstract

Current regulations on helmet certification drop tests insufficiently account for sustainable injuries to the human head. Main limitations are the use of a rigid head form and the single measurement of its resultant translational acceleration, whereas rotational accelerations are believed to be the cause of a major part of brain injuries. The objectives of this research project are to improve the head form in terms of anatomical detail and biofidelity on the one hand, and to develop a finite element model of the improved head form giving access to field parameters possibly correlated to injuries on the other hand.

A standard head form was studied and its geometry was determined using a three dimensional coordinate measuring device. Relevant anatomical structures of the human head were appointed and their mechanical properties have been investigated. Thes structures turned out to be the brain, the skull -including the neurocranium-, the chin and the falx and tentorium cerebri. Using this information an improved physical head form was designed. Als a finite element model of the improved physical head form has been developed, containing the relevant structures.

Representation of the relevant anatomical structures will yield more insight in possible injury mechanisms in the head under impact conditions, both for the physical and the numerical model. The finite element model proved to be suitable for numerical simulations and therefore contributes to a better understanding of the phenomena taking place in the head during impact.

The numerical model has to be validated against experimental data from the improved physical head form. In its turn this physical head form has to be evaluated using data from literature. Once validated, quantitative conclusions can be drawn from numerical simulations.

Acknowledgements

I hereby would like to thank everyone who contributed to this graduation project. In particular:

- Eric van den Bosch and Fons Sauren, for their valuable support and the pleasant cooperation during the project;
- Martijn Leensen, Dave Brands and Peter Bovendeerd, for their assistance and advice, and of course for the pleasant cooperation;
- George van de Molengraft, for all the work he put in producing the physical head form;
- The TNO Crash Safety Research Institute, for providing dummy head forms.

Finally I would like to thank my family and friends for their support and encouragement over the years.

Niels Plasmans